Isolation, Characterization, and Incorporation of Microfibrils and Microcrystals from *Typha domingensis* Pers. as Impact Strength Reinforcer of Polypropylene Matrix Composite Using Stearic Acid as Interfacial Modifier

Luisiana Morales-Zamudio,[a] Arturo López-Marure,[a] Margarita García-Hernández,[b] Francisco Rodríguez-González,[c] Sergio Flores-Gallardo,[d] and Erika López-Martínez [d]

Microcellulose has shown advantageous character as a reinforcement in polymeric materials and produces relatively light compounds with high specific properties. This research aimed to obtain microcellulose (crystals and fibers) from the macrophyte *Typha domingensis* for use as a polypropylene reinforcement material for impact strength improvement and to use stearic acid as an interfacial modifier (surfactant) between the polypropylene and cellulosic materials. A commercial cellulose was used to compare the effectiveness of the microcellulose isolated from the macrophyte. The results demonstrated the procedures were efficient at obtaining microcellulose. The analysis of the chemical composition indicated an increase in the α-cellulose content from 63.2% in the raw material to 97.9% in the bleached cellulose. The X-ray diffraction patterns showed that the chemical treatments changed the crystallinity. The thermogravimetric analysis revealed an increase in the thermal stability of the bleached cellulose compared with that of the raw material. The thermal stability of the macrophyte was higher than that of commercial cellulose. The scanning electron micrographs revealed the presence of longitudinal slits that favored interactions with the polymer matrix. The impact strength was greatly improved for the composites compared with the pure polypropylene.

Keywords: Typha domingensis; Cellulose fiber; Bleached pulp; Mechanical properties; Thermal properties; Crystallinity; Microstructure; Acid hydrolysis

Contact information: a: Instituto Politécnico Nacional, Centro de Investigación en Ciencia Aplicada y Tecnología Avanzada, Km. 14.5 Carretera Tampico-Puerto Industrial Altamira, Altamira, Tamaulipas, C.P. 89600, México; b: Tecnológico Nacional de México-Instituto Tecnológico de Ciudad Madero, Av. Primero de Mayo 1610, Los Mangos, 89460 Cd Madero, Tamaulipas, México; c: Centro de Investigación en Química Aplicada, Blvd. Enrique Reyna No. 140, Col. San José de los Cerritos, 25294 Saltillo, Coahuila, México; d: Centro de Investigación en Materiales Avanzados, Miguel de Cervantes 120, Complejo Industrial Chihuahua C.P. 31136 Chihuahua, Chih. México;
** Corresponding author: luisianamoza@hotmail.com*

INTRODUCTION

There has been an increasing environmental crisis caused by the use of nonrenewable, non-biodegradable materials such as polymer-based products. Their production recently has increased massively, generating more waste and affecting land and water resources. This has stimulated the development of new bio-based, green, and biodegradable materials from natural sources for various engineering applications (Kalia

et al. 2011a; Abdul Khalil *et al.* 2012; Thakur 2014; Thakur and Thakur 2014; Trache *et al.* 2016). Examples include a polymer matrix with incorporated fibers that can be found in either natural minerals or renewable plant raw materials. There are some advantages that natural fibers have over artificial ones, such as renewability, biodegradability, low cost, low density, and good mechanical properties (Spoljaric *et al.* 2009; Lavoine *et al.* 2012; Ng *et al.* 2015; Trache *et al.* 2016).

There has been a trend towards incorporating natural fibers such as cellulose into composites; cellulose is the most representative biomaterial, and it is abundantly found in plants as the main structural component that confers strength and stability to plant cell walls. Boldizar *et al.* (1987) showed that cellulose can be used as a reinforcement for polymeric materials. Interest in the isolation of cellulose from different resources, including pineapple leaves, abaca, pine, jute, and kenaf, for use as a polymer reinforcement has increased. Such interest is due to its high mechanical strength and stiffness combined with its renewability, biodegradability, and low weight (Beg and Pickering 2008; Rahman *et al.* 2009; Jahan *et al.* 2011; Nopparut and Amornsakchai 2016; Suharty *et al.* 2016).

Cellulose is a semicrystalline polymer comprised of crystalline (ordered) and amorphous (disordered) regions within the microfibril, where the individual cellulose molecule is considered to pass through several crystalline and amorphous regions. The native crystallinity degree is usually in the range of 40% to 70% and depends on the cellulose source and isolation method (Fengel and Wegener 1989; Habibi *et al.* 2010; Siqueira *et al.* 2010; Wertz *et al.* 2010). It is known that the crystal form cellulose (I) exists in nature in two main forms (triclinic Iα and monoclinic Iβ), from which cellulose II, III, and IV are derived (Fengel and Wegener 1989; Aulin 2009; Leppänen *et al.* 2009; Siqueira *et al.* 2010; Wertz *et al.* 2010).

To efficiently extract cellulose microcrystals, the determination of the chemical composition and removal of lignin and hemicellulose are essential. The chemical composition of the fibers can be determined according to TAPPI standards. One of the industrial separation methods for lignin and hemicellulose is the NaOH-anthraquinone (AQ) pulping process, which reduces the degradation rate and has a stabilization effect on cellulose macromolecules that is attributed to the AQ. Furthermore, AQ has been found to block the active groups of cellulose and decrease the rate of oxidation (Helmy and El-Motagali 1993). Usually bleaching treatments are performed to remove residual lignin and hemicellulose. After bleaching the cellulose and treating it with acid (sulfuric acid), it is possible to obtain microcrystalline cellulose (microcellulose). As hydrolysis occurs, sulfate groups are incorporated into the outer surface of cellulose (Dong and Gray 1997; Beck-Candanedo *et al.* 2005). After several centrifugation cycles that are sometimes combined with a dialysis method, neutralization takes place, often over long periods of time (Wang *et al.* 2007; Martínez-Sanz *et al.* 2011). However, some sulfate groups will remain because of the formation of ester groups, which leads to a lower degradation temperature of the cellulose (Wang *et al.* 2007). The thermal stability of cellulose microcrystals is important for their application as a reinforcement material, particularly for thermoplastics, because the processing temperature is usually high (Alemdar and Sain 2008).

A great variety of lignocellulosic materials can be used for microcrystal isolation, such as wood, vegetables, bacteria, and some macrophyte species (Beg and Pickering 2008; Rahman *et al.* 2009; Jahan *et al.* 2011; Martínez-Sanz *et al*. 2011; Khider *et al*. 2012; César *et al*. 2015; Nopparut and Amornsakchai 2016; Suharty *et al.* 2016). The present work studied and evaluated the potential of isolated microcellulose (crystals and fibers) from the macrophyte *Typha domingensis* Pers. to reinforce polypropylene (PP). This is the first work

in which the effects of incorporating different microcellulose acquisition stages from raw material up to the microcrystals are compared relative to the resulting impact strength reinforcement of polypropylene matrix composites. Because of the contrast between the polar nature of cellulose and the nonpolar nature of PP, stearic acid was used as an interfacial modifier (surfactant). To the knowledge of the authors, stearic acid has never been used as interface modifier in PP/microcellulose systems. This work is the first to study such an effect, based on the previous works of Hernandez *et al*. (2019). The hydrocarbon tail of the fatty acid provides compatibility with the polypropylene, and the acid functional group is capable of interactions with the microcellulose. The chemical composition of the fibers was determined for the raw material, cellulose after the pulping process, and bleached cellulose according to TAPPI standards. The raw materials, cellulose fibers (unbleached and bleached), cellulose microcrystals from *T. domingensis*, commercial cellulose, and cellulose microcrystals from the commercial cellulose were analyzed *via* Fourier transform infrared (FTIR) spectroscopy, wide-angle X-ray diffraction (XRD), scanning electron microscopy with energy dispersive spectroscopy (SEM/EDS), and thermogravimetric analysis (TGA) to determine and compare the properties, morphology, size, and thermal degradation behaviors. The composites were mechanically tested using the impact strength method and the fractured surfaces were studied through SEM observation. All the methodology implemented in this work is scalable to industrial level.

EXPERIMENTAL

Materials

Typha domingensis Pers., commonly known as southern cattail, was collected from "El Conejo" lagoon at Altamira, Tamaulipas, México, which is classified as wetland. This water body is close to the sea, and the infiltration of sea water brings sodium salts to the lagoon, which moreover receives industrial wastewater (Fierro 2009). The plant specimen was cut from the stem that protrudes from the water. The root was not studied in this research because it stores the greatest amount of metals and nutrients that were not of interest. The top part was sectioned and discarded, while the middle part was prepared and used as the raw material (César *et al.* 2015) using TAPPI T257 sp-14 (2014). The material was cut to a length of approximately 2.5 cm and dried at room temperature. The raw material was stored in hermetically sealed pouches to protect it from humidity. The chemicals and materials used in the present research were sodium hydroxide (99%) (Merck, Darmstadt, Germany), AQ (97%) (Sigma-Aldrich, St. Louis, MO, USA), sodium chloride (97%) (Reasol, Cd. Mexico, Mexico), glacial acetic acid (99%) (Fermont, Monterrey, Mexico), hydrogen peroxide (30% Purified) (Fermont, Monterrey, Mexico), sulfuric acid (99%) (Fermont, Monterrey, Mexico), commercial cellulose (J. T. Baker, Cd. Mexico, Mexico), ethanol (99.8%) (GC) (Sigma-Aldrich, Missouri, USA), stearic acid (98.5%) (Sigma-Aldrich, St. Louis, MO, USA), and Polypropylene Profax™ XH1760 (Indelpro Alpek, Tampico, Mexico).

Methods

Sample preparation

To obtain micron-sized fibers, the *T. domingensis* Pers. (raw material) was fed through a twin-screw extruder Omega 30 (Model ZSK 30, Steer, OH, USA) at a screw

speed of 100 rpm and at room temperature. After defibrillation, the material underwent a mechanical sieving process to obtain the desired particle size of 200-mesh.

Chemical composition

Few studies have evaluated the chemical composition from the raw material up to the bleached pulp to compare their content and determine the effectiveness of the delignification procedures during the different stages (Jonoobi *et al.* 2009). The samples were prepared according to TAPPI T264 cm-07 (2007). The moisture, ethanol extractives, water extractives, Klason lignin, α-cellulose, ash, NaOH extractives, and holocellulose contents were determined according to TAPPI T412 om-16 (2016), TAPPI T204 cm-17 (2017), TAPPI T207 cm-08 (2008), TAPPI T222 om-15 (2015), TAPPI T203 cm-09 (2009), TAPPI T211 om-16 (2016), TAPPI T212 om-12 (2012), and the holocellulose method by Wise *et al*. (1946), respectively. All of these characterizations were conducted in triplicate. Dixon's Q test and Student's t-test statistical analyses were performed using the XLSTAT-Pro 2018 software package (Addinsoft 2018.2 version, New York, NY, USA) to study the reliability of the data.

Pulping procedure

The fibers were cooked in a Parr reactor (5100 series and 4835 controllers, Parr Instrument Company, Moline, IL, USA). The cooking conditions are shown in Table 1. Subsequently, the pulps were washed until a neutral pH was obtained and then dried at room temperature.

Table 1. Conditions of the NaOH-AQ Pulping Process

Cooking Process	NaOH-AQ
NaOH	37%
AQ	0.1%
Liquor to Fiber Ratio	14:1
Temperature	160 °C
Cooking Time	90 min

Bleaching

To remove the residual lignin and other minor components, three-stage bleaching was performed, which was somewhat similar to the method reported by Jonoobi *et al.* (2009). Table 2 shows the conditions of the bleaching processes. The bleached pulps were washed with deionized water until a neutral pH was obtained and then dried at room temperature.

Table 2. Conditions of the Bleaching Process

Stage	B1	B2	B3
Reagents	Sodium Chloride (2%)	NaOH (1.5%)	Sodium Chloride (1.5%)
	Acetic Acid (3%)	H_2O_2 (1%)	Acetic Acid (3%)
Reagents to Fiber Ratio	11:1	11:1	11:1
Temperature	75 °C	75 °C	75 °C
Time	180 min	90 min	90 min

Cellulose microcrystals extraction

To isolate the microcrystals and compare the effectiveness of the procedures, acid hydrolysis was performed on the bleached *T. domingensis* cellulose and commercial cellulose with sulfuric acid concentrations of 24%, 34%, and 44% (w/w) at 60 °C for 30 min with continuous stirring. From the test results, a concentration of 34% sulfuric acid solution was adopted for acid hydrolysis. Concentrations above 34% promoted degradation of the samples, while 24% sulfuric acid was not sufficient for complete hydrolysis. The neutralization of the acid suspensions was done with continuous washing and centrifugation with deionized water until the suspensions were neutral (Roman and Winter 2004). Once neutrality was reached, a dispersion of cellulose microcrystals suspension was obtained *via* sonication for 30 min at room temperature. Then, the microcrystal suspension was dried into a powder form.

Before being incorporated to the polymer matrix, all the reinforcer materials obtained (microfibrils and microcrystals) were dried in an oven up to constant weight and subsequently hermetically storage to protect them from humidity.

Compounding of the composites

Composites containing PP and microcellulose (fibers and crystals) with and without stearic acid as an interfacial modifier were prepared in a Brabender twin screw extruder (D6/2, Brabender Instruments, Inc., Duisburg, Germany). The screw speed of the extruder was set to 50 rpm. The temperature profile was constant at 190 °C from the feed section to the die. The composites were processed in an injection molding machine (FNX80, Nissei, Shanghai, China) at 190 °C to mold the specimens to specific dimensions (63.5 mm × 12.7 mm × 3.0 mm) according to ASTM D256-10 (2010) (*ASTM International*) for the impact test. Table 3 shows the nomenclature and composition of the prepared composites.

Table 3. Nomenclature and Composition of the Prepared Composites

Without Interfacial Modifier		With 1.5 wt% of Interfacial Modifier	
Sample with Filler Contents of 10% w/w	**Nomenclature**	**Sample with Filler Contents of 10% w/w**	**Nomenclature**
PP	Polypropylene	PP/SA	Polypropylene with stearic acid
PP/RM	Polypropylene with raw material	PP/RM/SA	Polypropylene with raw material and stearic acid
PP/UF	Polypropylene with unbleached fibers	PP/UF/SA	Polypropylene, unbleached fibers and stearic acid
PP/BF	Polypropylene with bleached fibers	PP/BF/SA	Polypropylene with bleached fibers and stearic acid
PP/CMCTD	Polypropylene with cellulose microcrystals from *T. domingensis*	PP/CMCTD/SA	Polypropylene with cellulose microcrystals from *T. domingensis* and stearic acid
PP/CC	Polypropylene with commercial cellulose	PP/CC/SA	Polypropylene with commercial cellulose and stearic acid
PP/CMCCC	Polypropylene with cellulose microcrystals from commercial cellulose	PP/MCCC/SA	Polypropylene with cellulose microcrystals from commercial cellulose

Characterization

Wide-angle X-ray diffraction

The crystal structures of the fibers, commercial cellulose, and cellulose microcrystals were recorded with a wide-angle diffractometer (Bruker D8 Advance, Karlsruhe, Germany) equipped with a Lynx eye detector. The type of X-ray source used was CuKα with a wavelength of 1.5406 Å. The scattered radiation was detected in the angular range of 5° to 40° with a step size of 0.02° and a count time of 1 s per point. The crystallinity index (CrI) was calculated using the following equation (Segal *et al*. 1959),

$$CrI\ (\%) = [(I_{200} - I_{am}) / I_{200}] \times 100 \quad (1)$$

where *CrI* is the relative degree of crystallinity, I_{200} is the intensity of the (200) peak lattice diffraction at a 2θ of 22.8°, and I_{am} is the intensity of diffraction at a 2θ of 18°. The variable I_{200} represents both the crystalline and amorphous regions, while I_{am} represents only the amorphous region.

FTIR spectroscopy

To determine any changes in the functional groups that may have been caused by the treatments, FTIR spectroscopy was performed on an IRAffinity 1S (Shimadzu, Kyoto, Japan) spectrometer. The spectra were obtained by reflectance with attenuated total reflection (Quest model, Specac, Kent, England). The measurements were recorded in the 400 cm^{-1} to 4000 cm^{-1} range with a 4 cm^{-1} resolution and 64 scans for each sample.

Thermogravimetric analysis

Thermogravimetric analysis was done to characterize the thermal decomposition of the fibers after each treatment. The thermal stability data was obtained with a TA Instruments Q600 thermogravimetric analyzer (New Castle, DE, USA) under linear temperature conditions, where the temperature increased from 25 °C to 800 °C at a heating rate of 10 °C/min. An aluminium sample pan was used with an Argon atmosphere and gas flow rate of 50 mL/min. Derivative TG (DTG) curves expressed the weight loss rate as a function of the temperature.

Scanning electron microscopy with energy dispersive spectroscopy

A JEOL JSM-7610 FPlus Field Emission scanning electron microscope (JEOL Ltd., Tokyo, Japan) with an EDS detector was used to study the effect of the treatments on the fiber morphology and to study the carbon/oxygen atomic percentage of the microcellulose. All of the samples were sputter coated with gold to avoid charging (Tedpella, CA, USA). The fractured surface morphology of the Izod test composites were studied using a JEOL-JSM-7401F with a field emission gun at an accelerating voltage of 10 kV.

Mechanical properties

The composites were analyzed using notched Izod impact tests according to ASTM D256 (2010). A statistical analysis was performed using a one-way analysis of variance with a Tukey's honesty significant difference post hoc test to determine the differences between the individual batches. The differences were considered significant when $p \leq 0.05$. The statistical analyses were performed using the XLSTAT-Pro 2018 software package.

RESULTS AND DISCUSSION

Chemical Composition of the Fibers and Cellulose Pulps

Table 4 presents the content of the fibers and pulps before and after the chemo-mechanical treatments.

Table 4. Chemical Composition of the *T. domingensis* Pers.

Component	Raw Material	Unbleached Pulp	Bleached Pulp
Moisture (%)	10.17 ± 1.11	21.57 ± 0.46	6.11 ± 0.63
Ethanol Extractives (%)	11.13 ± 0.35	3.14 ± 0.07	1.50 ± 0.10
Water Extractives (%)	11.09 ± 0.49	9.87 ± 0.81	2.25 ± 0.69
Klason Lignin (%)	24.32 ± 0.70	1.87 ± 1.03	0.61 ± 0.01
Holocellulose (%)	77.67 ± 1.00	88.09 ± 0876	98.38 ± 0.27
α-cellulose (%)	63.20 ± 2.58	81.21 ± 1.22	97.87 ± 0.81
Hemicellulose (%)	14.47 ± 3.27	6.88 ± 1.72	0.51 ± 0.54
Ash (%)	7.34 ± 0.130	7.85 ± 0.14	0.33 ± 0.03
Solvent Extractives (%)	40.49 ± 0.49	14.93 ± 0.30	6.65 ± 0.31

The main constituents of plant cell walls are cellulose, hemicellulose, and lignin with lower contents of extractives, protein, starch, and inorganics. Table 4 shows that the α-cellulose content in the raw material was similar to that in jute, abaca, sisal, oil palm, and kenaf (Jonoobi *et al*. 2009; Faruk *et al*. 2012), which is lower than the content reported for *T. domingensis* from Brazil, flax, ramie, hemp, pineapple, and curauá (Faruk *et al*. 2012; César *et al*. 2015), and larger than the content in bagasse, bamboo, coir, wheat straw, rice husk, rice straw, and *T. domingensis* from Sudan (Faruk *et al*. 2012; Khider *et al*. 2012). The chemical composition and constituents vary from plant to plant and within different parts of the same plant. These values depend on the age, plant, soil and water body characteristics, nutrients, climatic conditions, and degradation process, which can influence the fiber structure and chemical composition (Xu 2010; Faruk *et al*. 2012).

The purification of cellulosic material by alkalization treatment is an essential stage because it helps to increase the crystallinity of the fibers (Majeed *et al*. 2013). The hemicellulose and lignin contents demonstrated that the NaOH-AQ pulping process was efficient, based on the reduction in the contents from the raw material (14.5% hemicellulose and 24.3% lignin) to the unbleached pulp (6.9% hemicellulose and 1.9% lignin). The elimination of hemicellulose is a crucial action, as it is undesired for reinforcement purposes because the initial decomposition of the cellulosic components takes place mostly in the hemicellulose. Moreover, the presence of lignin, wax, fats, extractives, and hydroxyl groups may hide the reactive sites (-OH groups), which are essential for fiber bonding with polymers (Jonoobi *et al*. 2009; Acharya *et al*. 2011). To remove the components other than α-cellulose from the unbleached pulp, a bleaching process was conducted. The bleached pulp showed that the percentage of α-cellulose increased up to 97.87%, while the residual components were reduced to a minimum percentage, which is important for subsequent acid hydrolysis, particularly because lignin coats the microfibril surface that is somewhat inaccessible to acid attack. The acid hydrolysis efficiency with less protective lignin could be higher by removing the amorphous phase, along with the crystalline phase (Ng *et al*. 2015). The reduction in the fiber diameter might have increased the aspect ratio by removing the cementing materials, which led to an increase in the surface area, resulting in a better fiber/matrix interface adhesion (Kalia *et al*. 2011b; Zainuddin *et al*. 2013).

The increase in the α-cellulose content from the raw material to the bleached pulp (from 63.2% to 97.87%) was a strong indicator of the potential of this macrophyte as a cellulose microcrystal source.

X-ray Diffraction

Figure 1 shows the diffraction patterns of the raw material, unbleached fibers, bleached fibers, commercial cellulose, and cellulose microcrystals from *T. domingensis* and commercial cellulose. The representative cellulose planes of (110) and (200), corresponded to the peaks at 2θ values of approximately 15° and 22°, respectively. These diffraction patterns showed the presence of cellulose type Iβ (monoclinic crystal structure), which is the dominant polymorph for higher plant cell wall cellulose (Moon *et al*. 2011).

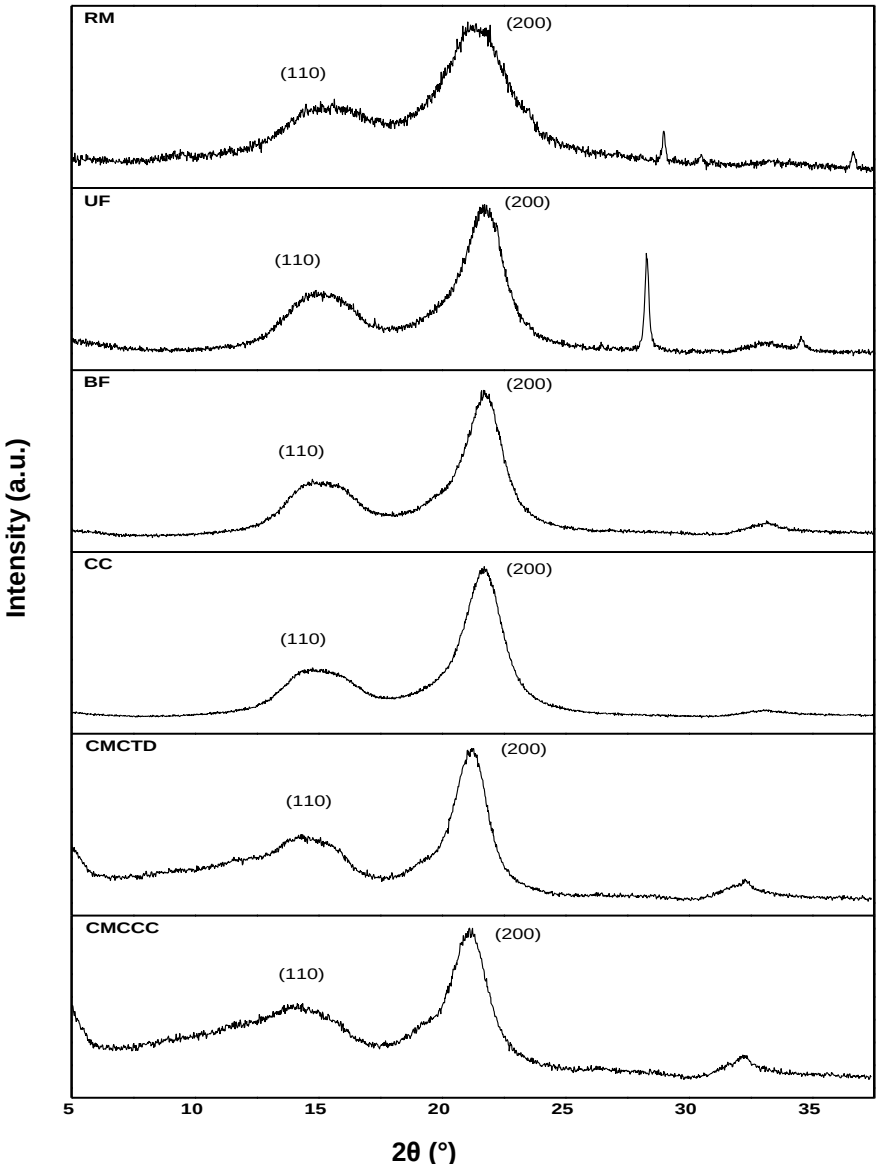

Fig. 1. XRD patterns of the raw material, unbleached fiber, bleached fiber, and commercial cellulose

The XRD patterns were also used to calculate the CrI, which was computed with Eq. 1. The CrI was 24.12%, 58.10%, 66.84%, 66.12%, 72.60%, and 68.72% for the raw material, unbleached fiber, bleached fiber, commercial cellulose, cellulose microcrystals from *T. domingensis*, and cellulose microcrystals from the commercial cellulose, respectively. These results confirmed the elimination of lignin and hemicellulose during the pulping and bleaching procedures, as well as the removal of the amorphous phase from the bleached cellulose during acid hydrolysis (Jonoobi *et al*. 2009; César *et al*. 2015).

FTIR Analysis

Fourier transform infrared spectroscopy was used to demonstrate the physical structure and functional groups in the lignocellulosic materials. The spectra of the untreated and treated fibers are shown in Fig. 2.

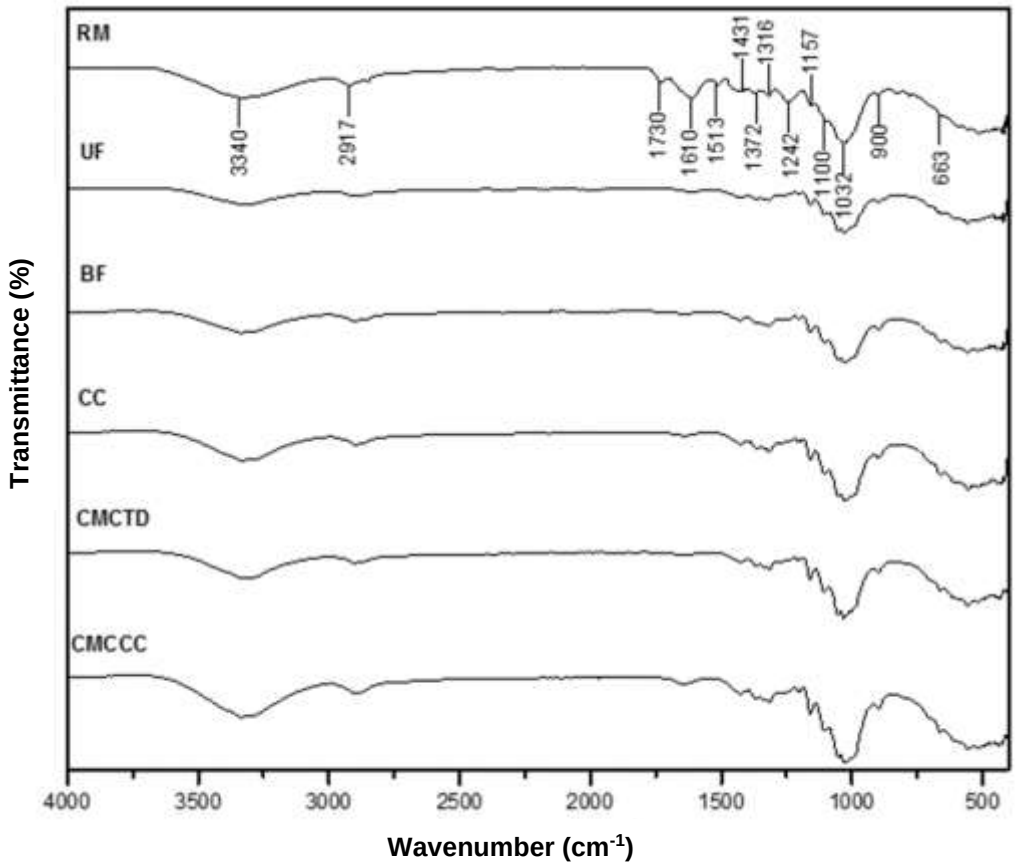

Fig. 2. Infrared spectra of the raw material, unbleached fiber, bleached fiber, commercial cellulose, cellulose microcrystals from *T. domingensis*, and cellulose microcrystals from the commercial cellulose

The broad absorption from 3000 cm^{-1} to 3600 cm^{-1} was ascribed to the stretching of H-bonded -OH groups (Jonoobi *et al*. 2009; Das *et al*. 2010; César *et al*. 2015). The peaks around 2900 cm^{-1} to 2800 cm^{-1} were due to the stretching of C-H (Das *et al*. 2010; César *et al*. 2015) and could have also been related to asymmetric CH_2 stretching of hemicellulose (César *et al*. 2015). The band located at 1730 cm^{-1} in the raw material was attributed to C=O stretching of the acetyl group in hemicellulose (Das *et al*. 2010; César *et al*. 2015) or to ferulic and *p*-coumaric acids of lignin and/or hemicellulose from the ester

linkage in carboxylic groups (Jonoobi *et al*. 2009). This band disappeared completely in the spectra of the treated cellulose fibers, which indicated the removal of lignin and most of the hemicellulose during the chemical treatments. The sharp band at 1610 cm^{-1} in the raw material was attributed to the bending mode of absorbed water in the cellulose (Jonoobi *et al*. 2009; Das *et al*. 2010; César *et al*. 2015). The intensity of the band at 1513 cm^{-1} was attributed to the C=C vibration from lignin and showed a considerable decrease from the raw material to the remaining samples, which indicated the large-scale removal of lignin (César *et al*. 2015). The absorbance from 1429 cm^{-1} to 1431 cm^{-1} was associated with CH_2 symmetric bending (Jonoobi *et al*. 2009). The bands observed in the range 1380 cm^{-1} to 1316 cm^{-1} in all of the samples were attributed to the bending vibration of C-H and C-O groups of the aromatic ring in polysaccharides (Jonoobi *et al*. 2009). There was another band associated with the effectiveness of the removal of lignin during the chemical treatments, specifically the C-O stretching of aryl groups in lignin, which were only present at 1242 cm^{-1} in the raw material (Jonoobi *et al*. 2009). The absorbance band at 1157 cm^{-1} from the antisymmetrical deformation of C-O-C bands appeared in all of the samples (Jonoobi *et al*. 2009). There was a growth in the intensity of the peaks that appeared at 1100 cm^{-1} and 1032 cm^{-1}, which were associated with -C-O-C- stretching of the β-1,4-glycosidic linkage in cellulose and the C-O stretching of cellulose, respectively. These bands were observed in the bleached fiber, commercial cellulose, and both cellulose microcrystals, which was attributed to the increase in the percentage of cellulosic components (Jonoobi *et al*. 2009; César *et al*. 2015). The vibration peak at 900 cm^{-1} was assigned to glycoside bonds, which are symmetrical in polysaccharides. Finally, the absorbance related to the torsion vibration of C-OH out-of-plane bending was present at 663 cm^{-1} (Das *et al*. 2010). Overall, the FTIR results corroborated the argument that efficient lignin removal occurred.

Thermal Analysis

The thermal degradation behavior was investigated with TGA measurements for all of the samples (from the raw material to the cellulose microcrystals, including the commercial cellulose). The TG thermograms of the raw material, unbleached fiber, bleached fiber, and commercial cellulose are shown in Fig. 3a and the thermograms of the cellulose microcrystals from the commercial cellulose and *T. domingensis* are shown in Fig. 3b. The DTG thermograms of the raw material, unbleached fiber, bleached fiber commercial cellulose, and microcrystals from *T. domingensis* and commercial cellulose are illustrated in Fig. 4.

These characterizations are indispensable for investigating the *T. domingensis* microcrystals as a reinforcing material of a polymeric matrix because of the relatively high temperatures required to process thermoplastic polymers (Boldizar *et al*. 1987; Roman and Winter 2004; Wang *et al*. 2007; Beg and Pickering 2008; Spoljaric *et al*. 2009; Ng *et al*. 2015). The first DTG peak of the thermogravimetric data of the microfibers for all of the cellulose samples indicated that initial decomposition took place mainly in the amorphous components. The thermogravimetric analysis for all of the samples showed that a small amount of weight loss at low temperatures (< 120 °C) took place that corresponded to the evaporation of absorbed water and low molecular weight compounds from the fibers (Roman and Winter 2004; César *et al*. 2015).

The weight loss was 5%, 4%, 2%, 2%, 3%, and 5% for the raw material, unbleached fiber, bleached fiber, commercial cellulose, cellulose microcrystals from *T. domingensis*, and cellulose microcrystals from the commercial cellulose, respectively. For the second event, the initial (T_{onset}) and end (T_{endset}) temperatures, weight loss (WL) percentage, and thermal decomposition temperature were determined by the maximum signal (T_d) and are shown in Table 5.

The DTG peak that appeared between 200 °C and 500 °C was attributed to the degradation of cellulose by various processes, such as depolymerization, dehydration, and decomposition of glycosyl units (César *et al*. 2015), which caused a better thermal stability for the unbleached and bleached fibers compared to that of the raw material. The maximum decomposition temperatures (T_{max}) of the unbleached fiber, bleached fiber, and raw materials were 348.7 °C, 357.8 °C, and 326.1 °C, respectively.

Moreover, the thermal stabilities of the unbleached and bleached fibers were superior to that of the commercial cellulose with a decomposition temperature of 330.6 °C. The thermal degradation of the raw material at a T_{max} of 326.1 °C was attributed to the decomposition of hemicellulose, while the decomposition at T_{max} for the other samples corresponded mainly to cellulose (Jonoobi *et al*. 2009). This was corroborated by the contents determined by the chemical composition characterization, as well by the XRD and FTIR analyses, where it was clearly visible that the proportion of cellulose increased as the amorphous component was removed by the mechanical and chemical processes. The higher content of residues in the raw material compared with the other samples was due to the presence of intrinsic components of the macrophyte, reported in the results of chemical composition, such as, ash, extractives, lignin, *etc*., which have a slow degradation rate (Jonoobi *et al*. 2009).

The DTG peak that appeared in the unbleached fiber above 500 °C was attributed to the oxidation and breakdown of the charred residues to lower molecular weight gaseous products (Roman and Winter 2004). While the stages of chemical treatments were performed to the bleached cellulose and microcrystals, the charred residues reduced as to be negligible, as can be observed in Fig. 4(a). The thermal decomposition of both microcrystals (*T. domingensis* and commercial) reduced the maximum decomposition temperature by 2 °C and 4 °C, respectively, compared with that of the fibers before hydrolysis. This was because of the sulfate groups incorporated into the outer surface of the cellulose during the hydrolysis process (Dong and Gray 1997; Beck-Candanedo *et al*. 2005; César *et al*. 2015).

Even though a neutral pH was reached after hydrolysis, some sulfate groups still remained because of the formation of ester groups, which led to a lower degradation temperature of the cellulose (Wang *et al*. 2007). However, the T_{max} for the bleached fibers was 357.8 °C. This was an increase of approximately 32 °C compared with that of the raw material, which had a T_{max} of 326.1 °C. A high T_{max} is required to use a material as reinforcement in composite materials.

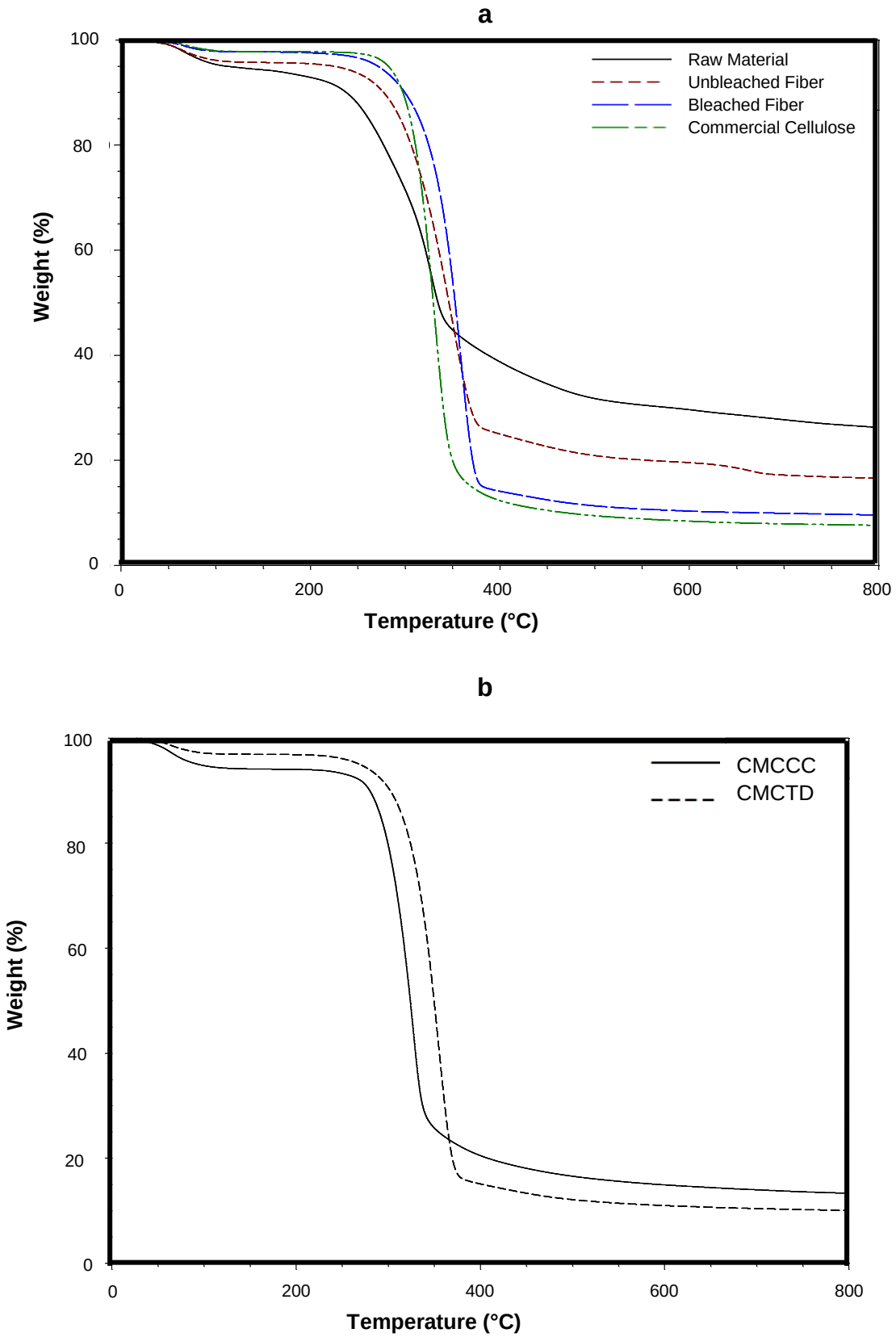

Fig. 3. TG curves for the (a) raw material, unbleached fiber, bleached fiber, and commercial cellulose, and (b) cellulose microcrystals from the commercial cellulose and *T. domingensis*

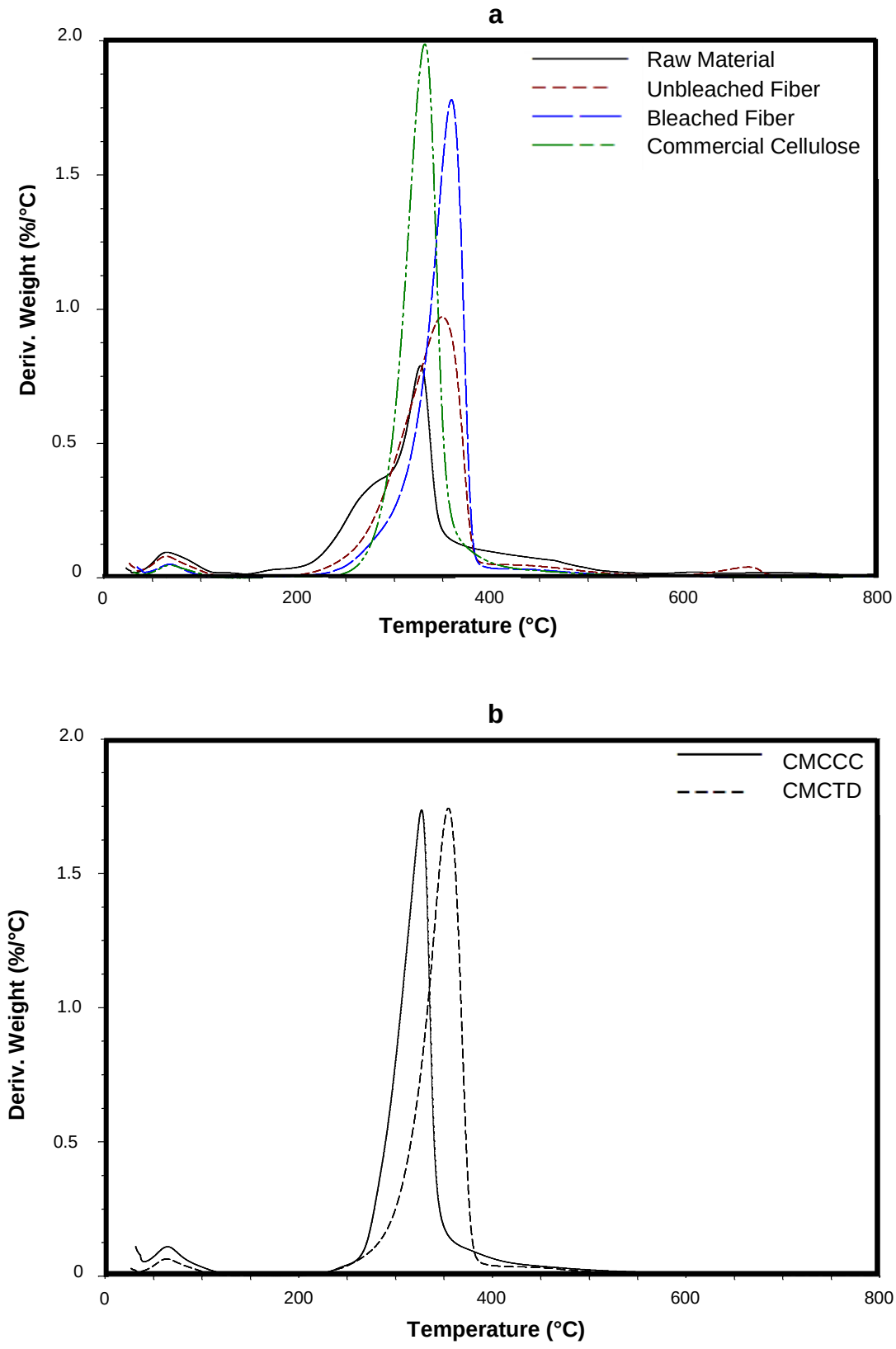

Fig. 4. DTG curves for the (a) raw material, unbleached fiber, bleached fiber, and commercial cellulose, and (b) cellulose microcrystals from the commercial cellulose and *T. domingensis*

Table 5. Thermal Properties (Second Thermal Event)

	RM	UF	BF	CC	CMCTD	CMCCC
T_{onset} (°C)	150	220	240	260	250	250
T_{endset} (°C)	550	400	400	400	450	450
T_d (°C)	326.14	348.70	357.78	330.55	355.06	326.27
WL (%)	64.16	75.77	83.774	86.50	84.57	76.88

Morphological Characterization

The morphological characteristics of all of the microfibers and microcrystals were evaluated by SEM analysis. Figure 5a shows the *T. domingensis* as a raw material before the chemical treatments. There was a superficial layer with a high percentage of extractives on the fibers, which was similar to observations in literature (Mathew *et al.* 2011). Figure 5b shows the unbleached fibers. A defined fiber surface was observed because of the high removal of extractives by the NaOH-AQ treatments. The bleached fibers confirmed the elimination of most of the components in the raw material by exposing neat longitudinal slits on the fiber surface that increased the surface roughness and provided sites for mechanical interlocking. Furthermore, the increased contact area improved the bonding with the polymer matrix, as shown in Fig. 5c. These observations of the chemically treated materials were consistent with the observations reported in the literature (Cerqueira *et al*. 2011; César *et al*. 2015; Sullins *et al*. 2017). Figure 5d shows the microcrystals from *T. domingensis*. No changes occurred to the surface and the microcrystals maintained the same longitudinal slits visible on the bleached fibers. However, it was clear that the reduction in the length increased the surface contact area. An increased surface area of a treated fiber surface results in increased bonding with thermoplastic polymer matrices (Sullins *et al*. 2017). The commercial microcrystals are illustrated in Fig. 5e and it was observed that there was not a defined shape, homogeneous size, or flat surface compared with the microcrystals from *T. domingensis* obtained under the same chemical treatments. The differences between the cellulose microcrystals could have been because of the different cellulose sources.

Energy dispersive spectroscopy was conducted on the bleached fibers and cellulose microcrystals from *T. domingensis* and commercial cellulose to measure the atomic percentage of the carbon/oxygen ratio before and after acid hydrolysis. This was done because of the reduction in the thermal stability of the microcrystals, which was related to the incorporation of sulfate groups. Figure 6a shows the carbon/oxygen atomic content of the bleached fibers, while Figs. 6b and 6c show the carbon/oxygen atomic contents for the cellulose microcrystals from *T. domingensis* and commercial cellulose, respectively. Table 6 summarizes the atomic percentage and carbon/oxygen ratios for the bleached fibers and cellulose microcrystals from *T. domingensis* and commercial cellulose. There was a clear increase in the oxygen content after acid hydrolysis because of the oxygen atoms in the sulfate groups. This corroborated the reduction in the thermal stability of the cellulose microcrystals from *T. domingensis* and commercial cellulose. The previous study by Guerrero *et al*. (2001) focused on the carbon/oxygen ratios determined by the EDS technique, which were used to identify different composition blends.

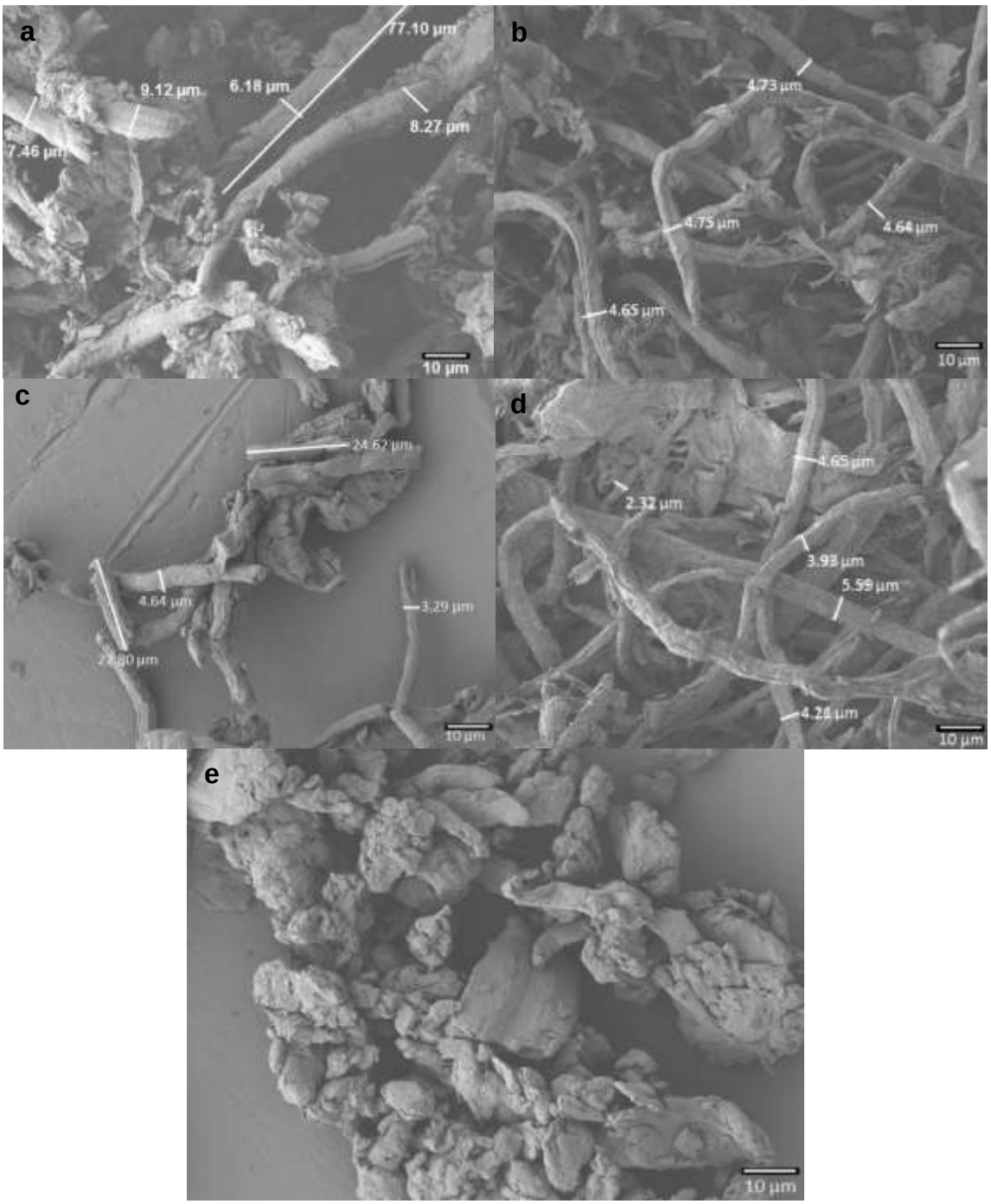

Fig. 5. SEM photographs of the (a) raw material, (b) unbleached fibers, (c) bleached fibers, (d) cellulose microcrystals from *T. domingensis*, and (e) cellulose microcrystals from the commercial cellulose

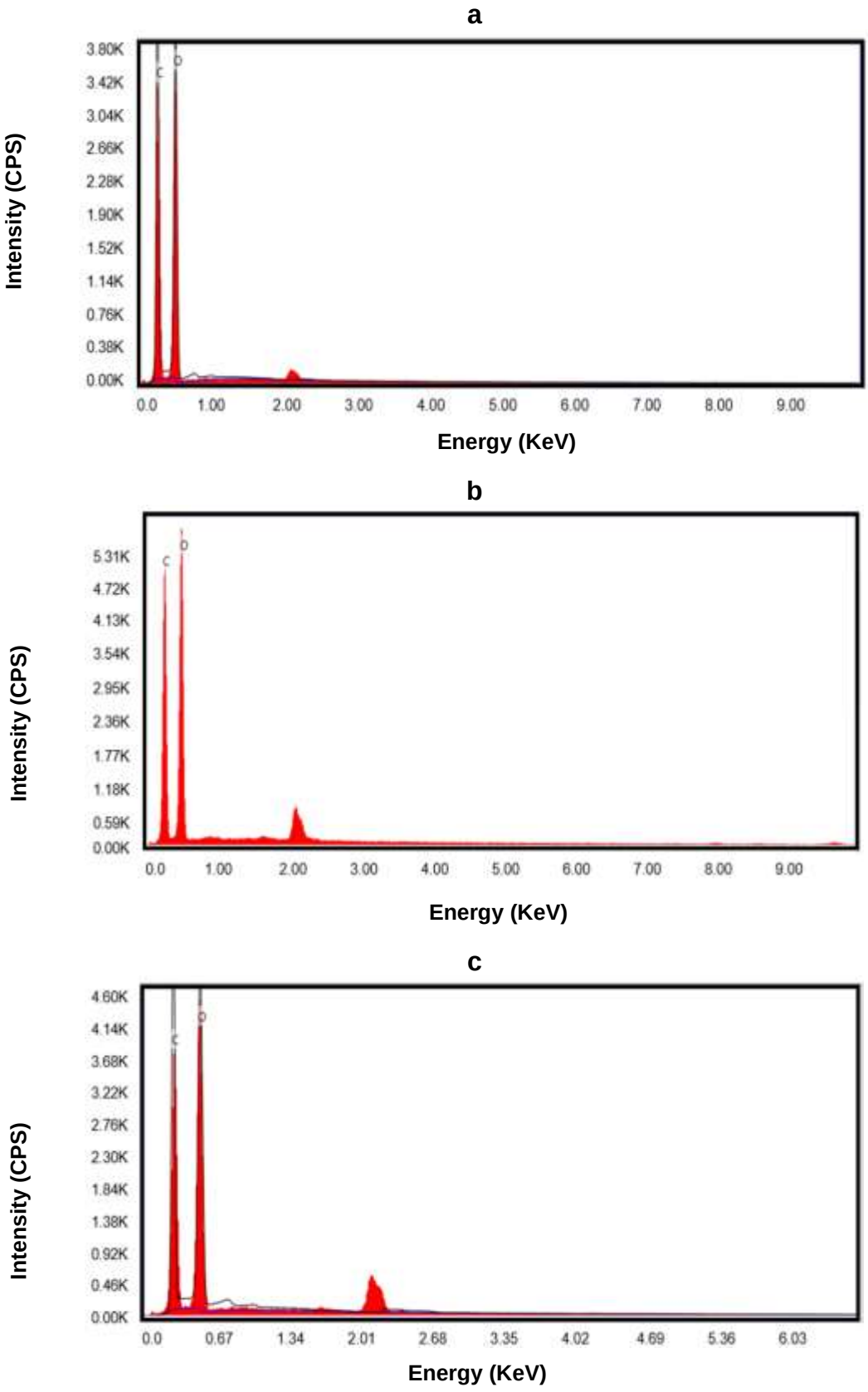

Fig. 6. EDS graphs for the (a) bleached fibers, (b) cellulose microcrystals from *T. domingensis*, and (c) cellulose microcrystals from the commercial cellulose

Table 6. Atomic Percentage and Carbon/Oxygen Ratio

Material	Atomic % of Carbon	Atomic % of Oxygen	Carbon/Oxygen Ratio
BF	54.96	45.04	0.82
CMCTD	53.12	46.88	0.88
CMCCC	52.76	47.24	0.90

Mechanical Properties

The mechanical properties of the studied composites are given in Table 7. The composites showed distinct impact strengths with the incorporation of the different chemically treated fibers, as well as when stearic acid was added as an interfacial modifier compared with the composites without stearic acid. The effects were attributed to the different fiber-matrix interactions. For all of the composites, the impact strength increased compared to that of the pure PP. The composites had a maximum impact strength increase of 36% with the interfacial modifier (PP/BF/SA) and a maximum increase of 21% without the interfacial modifier (PP/BF). The large increase for the composites with stearic acid could have been because bonding formed between the carboxylic groups and OH positions on the cellulose. This resulted in a better interphase between the fiber-matrix compared with the composites without the interfacial modifier. These results agreed with the results of Ummartyotin and Pechyen (2016), as well as Sullins *et al*. (2017), who utilized PP-g-MA (maleic anhydride) as a coupling agent and reported an increase in the studied mechanical properties that was attributed to the interaction between the coupling agent and microcellulose. This improved the compatibility with the polymer matrix after chemical modification of the cellulose surface. When stearic acid was incorporated during the extrusion as an interfacial modifier, the temperatures used during the extrusion process favor the formation of an ester bond with the microcellulose, while a physical interaction took place on the polymer, which improved the interactions between the polymer matrix and cellulose fiber reinforcement.

Table 7. Impact Strength of the PP Composites

	Impact Strength (J/m)	
Composite	Without Interfacial Modifier	With 1.5 wt.% Interfacial Modifier
PP	26.57 ± 1.08	35.00 ± 1.21
PP/RM	30.88 ± 1.55	33.41 ± 0.88
PP/UF	31.40 ± 1.26	33.79 ± 1.24
PP/BF	32.16 ± 0.71	36.16 ± 1.29
PP/CMCTD	30.54 ± 1.92	31.33 ± 0.28
PP/CC	28.36 ± 1.84	31.66 ± 2.48
PP/CMCCC	27.30 ± 1.25	31.17 ± 1.42

Morphological Characterization of the Fractured Surface Composites

The fractured surface morphologies of the Izod impact test specimens PP/RW/SA, PP/BF, and PP/BF/SA are illustrated in Figs. 7a, 7b, and 7c, respectively. Figure 7a shows the behavior of the raw material fibers, where it was clearly visible that the high stretching of the fiber conferred toughness to the polymer matrix and improved its impact resistance.

The composites containing bleached fibers with and without stearic acid were chosen because they had the highest impact resistance. Figure 7b shows that the sample with stearic acid had a better distribution of fibers within the polymeric matrix than the sample without the interface modifier. Additionally, the surfactant contributed to good

adhesion between the fibers and polymer and was the reason for the highest improvement in the impact resistance. Figure 7c shows that the fibers of the composites without stearic acid tended to agglomerate. Even though agglomeration creates fragile zones, the good mechanical properties of the fibers and its roughness (longitudinal slits exposed on the bleached fibers) improved the impact resistance of the polymer. These results again showed the potential of these fibers as polymer reinforcement and the efficiency of stearic acid as a surfactant between the polymeric component and cellulose fibers.

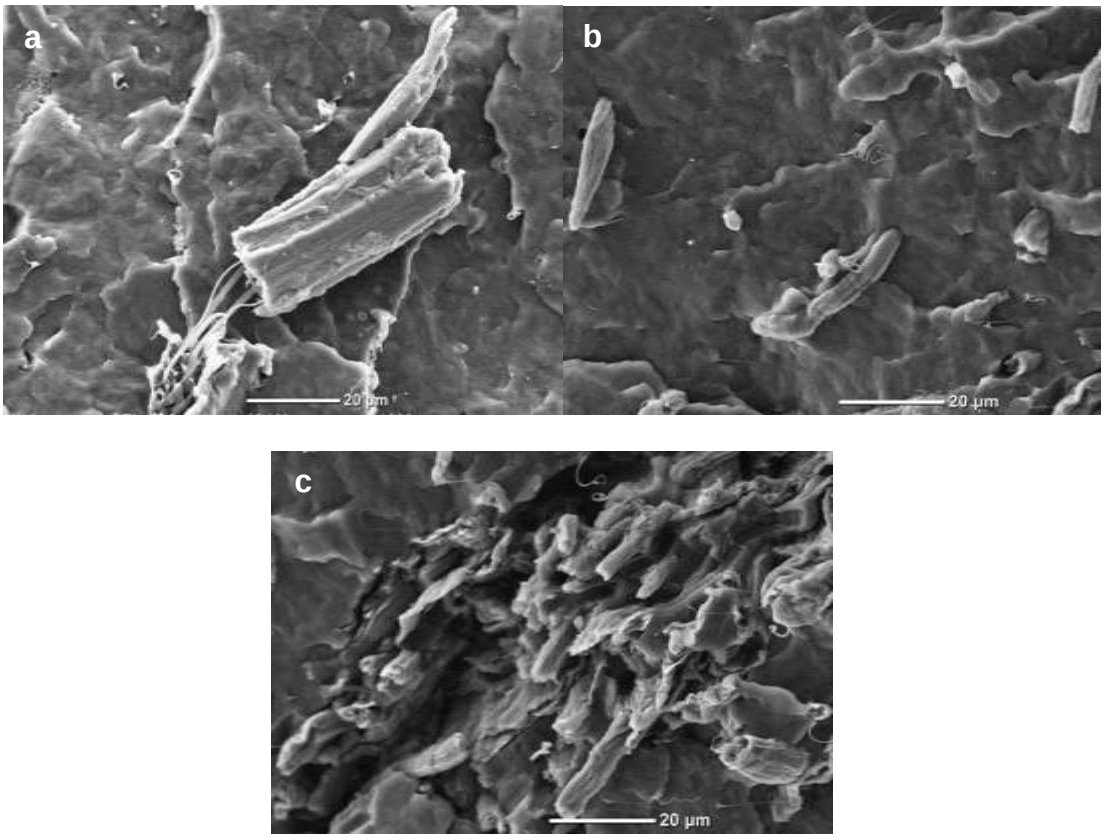

Fig. 7. SEM photographs of the fractured surface of (a) PP/RW/SA, (b) PP/BF, and (c) PP/BF/SA

CONCLUSIONS

1. The chemical content of the cellulose increased from 63.2% (raw material) up to 97.9% after the chemical treatments were applied. The type of obtained isolated cellulose was Type I, which was determined by means of XRD analysis.
2. The chemical treatments successfully removed the amorphous components present in the raw material. The absorption bands related to lignin and hemicellulose components in the FTIR spectra were not observed in the spectra of the unbleached and bleached cellulose.
3. The XRD analysis indicated a higher crystallinity for the chemically treated fibers, and the highest crystallinity was found in the cellulose microcrystal from *T. domingensis*.

Overall, the crystallinity increased from 24.1% in the raw material to 72.6% in the cellulose microcrystals from *T. domingensis*.

4. The TGA revealed that the thermal stability increased in the fibers that underwent the chemo-mechanical treatments. This was due to the removal of hemicellulose and lignin, as well as the increase in the crystallinity during processing.
5. The cellulose obtained in the laboratory had a better thermal stability compared with the commercial cellulose. The decomposition of the commercial cellulose started at 330.6 °C, whereas decomposition of the cellulose obtained from *T. domingensis* started at 357.8 °C with a weight loss of 50 wt%. The raw material showed the lowest thermal stability with a T_{max} of 326.1 °C.
6. The addition of stearic acid to the PP/cellulose fibers system had a positive effect on the impact strength as well as a strong effect at the interface. The interfacial modifier generated interactions between the components, which led to a better wetting of the polymer and better dispersive mixing (size of the fibers was diminished).
7. The largest improvement in the impact strength of the composites was found with the bleached fibers from *T. domingensis* (with and without surfactant). This was an effect of the neat surface area and exposed slits of the microfibers that contributed to a high contact surface and was also because of the presence of stearic acid.
8. The increase in the impact strength demonstrated the potential of *T. domingensis* microcellulose as reinforcement in polymers, with an increase of up to 36% with the interfacial modifier (PP/BF/SA) compared with that of the pure PP.
9. From the SEM results, the cellulose microcrystals from the commercial cellulose did not show a defined shape to determine an L/D (length/diameter) ratio. The size was bigger than that obtained with the cellulose microcrystals from *T. domingensis*. The SEM images of the commercial cellulose showed smoother fibers on the surface, which caused poor bonding with the polymer. The microfibers and microcrystals from *T. domingensis* had exposed rough surfaces, which favored interactions/bonding with the polymer matrix.

ACKNOWLEDGMENTS

The authors are grateful to the Instituto Politecnico Nacional, Centro de Investigación en Ciencia Aplicada y Tecnología Avanzada campus Altamira (CICATA) for the support in developing the present research; to Consejo Nacional en Ciencia y Tecnología (CONACYT) for the Ph.D. scholarship; to Centro de investigación en Química Aplicada (CIQA) and their technicians Josue de Jesus Campos Oyervides, Maria Guadalupe Mendez Padilla, Rosario Rangel, Juan Francisco Zendejo Rodriguez, Maria Concepción Gonzalez, and Rodrigo Cedillo García for their support with the mechanical properties characterization and preparation of the samples; to Tecnológico Nacional de México-Instituto Tecnológico de Ciudad Madero (ITCM) and Centro de Investigación en Materiales Avanzados (CIMAV) for the facilities and equipment; to Wilber Antunez Flores and Ernesto Guerrero Lestarjette from Laboratorio Nacional de Nanotecnología of CIMAV for their support with the SEM and XRD characterizations; and to Luis de la Torre Sáenz

and Daniel Lardizábal Gutierrez from CIMAV for their support with the FTIR and TGA characterizations.

REFERENCES CITED

Abdul Khalil, H. P. S., Bhat, A. H., and Yusra, A. F. I. (2012). "Green composites from sustainable cellulose nanofibrils: A review," *Carbohyd. Polym.* 87(2), 963-979. DOI: 10.1016/j.carbpol.2011.08.078

Acharya, S. K., Mishra, P., and Mehar, S. K. (2011). "Effect of surface treatment on the mechanical properties of bagasse fiber reinforced polymer composite," *BioResources* 6(3), 3155-3165. DOI: 10.15376/biores.6.3.3155-3165

Alemdar, A., and Sain, M. (2008). "Isolation and characterization of nanofibers from agricultural residues – Wheat straw and soy hulls," *Bioresource Technol.* 99(6), 1664-1671. DOI: 10.1016/j.biortech.2007.04.029

ASTM D256-10 (2010). "Standard test method for determining the Izod pendulum impact resistence of plastics," ASTM International, West Conshohocken, PA.

Aulin, C. (2009). *Novel Oil Resistant Cellulosic Materials (Pulp and Paper Technology)*, Ph.D. Thesis, KTH Royal Institute of Technology, Stockholm, Sweden.

Beck-Candanedo, S., Roman, M., and Gray, D. G. (2005). "Effect of reaction conditions on the properties and behavior of wood cellulose nanocrystal suspensions," *Biomacromolecules* 6(2), 1048-1054. DOI: 10.1021/bm049300p

Beg, M. D. H., and Pickering, K. L. (2008). "Mechanical performance of kraft fibre reinforced polypropylene composites: Influence of fibre length, fibre beating and hygrothermal ageing," *Compos. Part A-Appl. S.* 39(11), 1748–1755. DOI: 10.1016/j.compositesa.2008.08.003

Boldizar, A., Klason, C., Kubát, J., Näslund, P., and Saha, P. (1987). "Prehydrolyzed cellulose as reinforcing filler for thermoplastics," *Int. J. Polym. Mater.* 11(4), 229–262. DOI: 10.1080/00914038708078665

Cerqueira, E. F., Baptista, C. A. R. P., and Mulinari, D. R. (2011). "Mechanical behaviour of polypropylene reinforced sugarcane bagasse fibers composites," *Procedia Engineer.* 10, 2046-2051. DOI: 10.1016/j.proeng.2011.04.339

César, N. R., Pereira-da-Silva, M. A., Botaro, V. R., and De Menezes, A. J. (2015). "Cellulose nanocrystals from natural fiber of the macrophyte *Typha domingensis*: Extraction and characterization," *Cellulose* 22(1), 449-460. DOI: 10.1007/s10570-014-0533-7

Das, K., Ray, D., Bandyopadhyay, N. R., and Sengupta, S. (2010). "Study of the properties of microcrystalline cellulose particles from different renewable resources by XRD, FTIR, nanoindentation, TGA and SEM," *J. Polym. Environ.* 18(3), 355-363. DOI: 10.1007/s10924-010-0167-2

Dong, X. M., and Gray, D. G. (1997). "Effect of counterions on ordered phase formation in suspensions of charged rodlike cellulose crystallites," *Langmuir* 13(8), 2404-2409. DOI: 10.1021/la960724h

Faruk, O., Bledzki, A. K., Fink, H.-P., and Sain, M. (2012). "Biocomposites reinforced with natural fibers: 2000–2010," *Prog. Polym. Sci.* 37(11), 1552-1596. DOI: 10.1016/j.progpolymsci.2012.04.003

Fengel, D. and Wegener, G. (1989). "Wood – Chemistry, Ultrastructure, Reactions", *J. Polym. Sci. Pol. Lett.* 23(11), 601-602. DOI: 10.1002/pol.1985.130231112

Fierro, A. (2009). "Indicadores funcionales y estructurales para evaluar el estado de conservación de humedales costeros en el sur de Tamaulipas," *CienciaUAT*, 4(1), 61-63. Available: //www.redalyc.org/articulo.oa?id=441942917001

Guerrero, C., Lozano, T., González, V., and Arroyo, E. (2001). "Properties and morphology of poly(ethylene terephthalate) and high-density polyethylene blends," *J. Appl. Polym. Sci.* 82(6), 1382-1390. DOI: 10.1002/app.1975

Habibi, Y., Lucia, L. A., and Rojas, O. J. (2010). "Cellulose nanocrystals: Chemistry, self -assembly, and applications," *Chem. Rev.* 110(6), 3479-3500. DOI: 10.1021/cr900339w

Helmy, S. A., and El-Motagali, H. A. A. (1993). "Studies on the alkaline degradation of cellulose. III. Alkaline treatment in presence of anthraquinone," *Polym. Degrad. Stabil.* 40(1), 9-12. DOI: 10.1016/0141-3910(93)90183-J

Hernandez, Y., Lozano, T., Morales-Cepeda, A., Navarro-Pardo, F., E Ángeles, M., Morales-Zamudio, L., Melo-Banda, J.A., Sánchez-Valdés, S., Martínez, G., Rodríguez, F. (2019). "Stearic acid as interface modifier and lubricant agent of the system: Polypropylene/calcium carbonate nanoparticles," *Polymer Engineering and Science*. 1-7. DOI: 10.1002/pen.25053

Jahan, M. S., Saeed, A., He, Z., and Ni, Y. (2011). "Jute as raw material for the preparation of microcrystalline cellulose," *Cellulose* 18(2), 451-459. DOI: 10.1007/s10570-010-9481-z

Jonoobi, M., Harun, J., Shakeri, A., Misra, M., and Oksman, K. (2009). "Chemical composition, crystallinity, and thermal degradation of bleached and unbleached kenaf bast (*Hibiscus cannabinus*) pulp and nanofibers," *BioResources* 4(2), 626-639. DOI: 10.15376/biores.4.2.626-639

Kalia, S., Dufresne, A., Cherian, B. M., Kaith, B. S., Avérous, L., Njuguna, J., and Nassiopoulos, E. (2011a). "Cellulose-based bio- and nanocomposites: A review," *Int. J. Polym. Sci.* 2011, 1-35. DOI: 10.1155/2011/837875

Kalia, S., Kaith, B. S., and Kaur, I. (2011b). *Cellulose Fibers: Bio- and Nano-polymer Composites: Green Chemistry and Technology*, Springer-Verlag, Berlin, Germany.

Khider, T. O., Omer, S., and Taha, O. (2012). "Alkaline pulping of *Typha domingensis* stems from Sudan," *World Applied Sciences Journal* 16(3), 331-336.

Lavoine, N., Desloges, I., Dufresne, A., and Bras, J. (2012). "Microfibrillated cellulose – Its barrier properties and applications in cellulosic materials: A review," *Carbohyd. Polym.* 90(2), 735-764. DOI: 10.1016/j.carbpol.2012.05.026

Leppänen, K., Andersson, S., Torkkeli, M., Knaapila, M., Kotelnikova, N., and Serimaa, R. (2009). "Structure of cellulose and microcrystalline cellulose from various wood species, cotton and flax studied by X-ray scattering," *Cellulose* 16(6), 999-1015. DOI: 10.1007/s10570-009-9298-9

Majeed, K., Jawaid, M., Hassan, A., Abu Bakar, A., Abdul Khalil, H. P. S., Salema, A. A., and Inuwa, I. (2013). "Potential materials for food packaging from nanoclay/ natural fibres filled hybrid composites," *Mater. Design* 46, 391-410. DOI: 10.1016/j.matdes.2012.10.044

Martínez-Sanz, M., López-Rubio, A., and Lagaron, J. M. (2011). "Optimization of the nanofabrication by acid hydrolysis of bacterial cellulose nanowhiskers," *Carbohyd. Polym.* 85(1), 228-236. DOI: 10.1016/j.carbpol.2011.02.021

Mathew, L., Joshy, M. K., and Joseph, R. (2011). "Isora fibre: A natural reinforcement for the development of high performance engineering materials," in: *Cellulose*

Fibers: Bio- and Nano-polymer Composites, Green Chemistry and Technology, S. Kalia, B. S Kaith, and I. Kaur (eds.), Springer-Verlag, Berlin, Germany, pp. 291-324.

Moon, R. J., Martini, A., Nairn, J., Simonsen, J., and Youngblood, J. (2011). "Cellulose nanomaterials review: Structure, properties and nanocomposites," *Chem. Soc. Rev.* 40(7), 3941-3994. DOI: 10.1039/C0CS00108B

Ng, H.-M., Sin, L. T., Tee, T.-T., Bee, S.-T., Hui, D., Low, C.-Y., and Rahmat, A. R. (2015). "Extraction of cellulose nanocrystals from plant sources for application as reinforcing agent in polymers," *Compos. Part B-Eng.* 75, 176-200. DOI: 10.1016/j.compositesb.2015.01.008

Nopparut, A., and Amornsakchai, T. (2016). "Influence of pineapple leaf fiber and its surface treatment on molecular orientation in, and mechanical properties of, injection molded nylon composites," *Polym. Test.* 52, 141-149. DOI: 10.1016/j.polymertesting.2016.04.012

Rahman, M. R., Huque, M. M., Islam, M. N., and Hasan, M. (2009). "Mechanical properties of polypropylene composites reinforced with chemically treated abaca," *Compos. Part A-Appl. S.* 40(4), 511-517. DOI: 10.1016/j.compositesa.2009.01.013

Roman, M., and Winter, W. T. (2004). "Effect of sulfate groups from sulfuric acid hydrolysis on the thermal degradation behavior of bacterial cellulose," *Biomacromolecules* 5(5), 1671-1677. DOI: 10.1021/bm034519

Segal, L., Creely, J. J., Martin, Jr., A. E., and Conrad, C. M. (1959). "An empirical method for estimating the degree of crystallinity of native cellulose using the X-ray diffractometer," *Text. Res. J.* 29(10), 786-794. DOI: 10.1177/004051755902901003

Siqueira, G., Bras, J., and Dufresne, A. (2010). "Cellulosic bionanocomposites: A review of preparation, properties and applications," *Polymer* 2(4), 728-765. DOI: 10.3390/polym2040728

Spoljaric, S., Genovese, A., and Shanks, R. A. (2009). "Polypropylene–microcrystalline cellulose composites with enhanced compatibility and properties," *Compos. Part A-Appl. S.* 40(6-7), 791-799. DOI: 10.1016/j.compositesa.2009.03.011

Suharty, N. S., Ismail, H., Diharjo, K., Handayani, D. S., and Firdaus, M. (2016). "Effect of kenaf fiber as a reinforcement on the tensile, flexural strength and impact toughness properties of recycled polypropylene/halloysite composites," *Procedia Chem.* 19, 253-258. DOI: 10.1016/j.proche.2016.03.102

Sullins, T., Pillay, S., Komus, A., and Ning, H. (2017). "Hemp fiber reinforced polypropylene composites: The effects of material treatments," *Compos. Part B-Eng.* 114, 15-22. DOI: 10.1016/j.compositesb.2017.02.001

TAPPI T203 cm-09 (2009). "Alpha-, beta- and gamma-cellulose in pulp," TAPPI Press, Atlanta, GA.

TAPPI T204 cm-17 (2017). "Solvent extractives of wood and pulp," TAPPI Press, Atlanta, GA.

TAPPI T207 cm-08 (2008). "Water solubility of wood and pulp," TAPPI Press, Atlanta, GA.

TAPPI T211 om-16 (2016). "Ash in wood, pulp, paper and paperboard: Combustion at 525 °C," TAPPI Press, Atlanta, GA.

TAPPI T212 om-12 (2012). "One percent of sodium hydroxide solubility of wood and pulp," TAPPI Press, Atlanta, GA.

TAPPI T222 om-15 (2015). "Acid-insoluble lignin in wood and pulp," TAPPI Press, Atlanta, GA.

TAPPI T257 sp-14 (2014). "Sampling and preparing wood for analysis," TAPPI Press, Atlanta, GA.

TAPPI T264 cm-07 (2007). "Preparation of wood for chemical analysis," TAPPI Press, Atlanta, GA.

TAPPI T412 om-16 (2016). "Moisture in pulp, paper and paperboard," TAPPI Press, Atlanta, GA.

Thakur, V. K. (2014). *Nanocellulose Polymer Nanocomposites: Fundamentals and Applications*, John Wiley & Sons, Hoboken, NJ.

Thakur, V. K., and Thakur, M. K. (2014). "Processing and characterization of natural cellulose fibers/thermoset polymer composites," *Carbohyd. Polym.* 109, 102-117. DOI: 10.1016/j.carbpol.2014.03.039

Trache, D., Hussin, M. H., Chuin, C. T. H., Sabar, S., Fazita, M. R. N., Taiwo, O. F. A., Hassan, T. M., and Haafiz, M. K. M. (2016). "Microcrystalline cellulose: Isolation, characterization and bio-composites application—A review," *Int. J. Biol. Macromol.* 93(Part A), 789-804. DOI: 10.1016/j.ijbiomac.2016.09.056

Ummartyotin, S., and Pechyen, C. (2016). "Microcrystalline-cellulose and polypropylene based composite: A simple, selective and effective material for microwavable packaging," *Carbohyd. Polym.* 142, 133-140. DOI: 10.1016/j.carbpol.2016.01.020

Wang, N., Ding, E., and Cheng, R. (2007). "Thermal degradation behaviors of spherical cellulose nanocrystals with sulfate groups," *Polymer* 48(12), 3486-3493. DOI: 10.1016/j.polymer.2007.03.062

Wertz, J.-L., Bédué, O., and Mercier, J. P. (2010). *Cellulose Science and Technology*, EPFL Press, Lausanne, Switzerland.

Wise, L. E., Murphy, M., and D'Adieco, A. A. (1946). "Chlorite holocellulose, its fractionation and bearing on summative wood analysis and studies on the hemicelluloses," *Paper Trade Journal* 122(2), 35-43.

Xu, F. (2010). "Chapter 2 - Structure, ultrastructure, and chemical composition," in: *Cereal Straw as a Resource for Sustainable Biomaterials and Biofuels*, R.-C. Sung (ed.), Elsevier, Oxford, UK, pp. 121-131.

Zainuddin, S. Y. Z., Ahmad, I., Kargarzadeh, H., Abdullah, I., and Dufresne, A. (2013). "Potential of using multiscale kenaf fibers as reinforcing filler in cassava starch-kenaf biocomposites," *Carbohyd. Polym.* 92(2), 2299-2305. DOI: 10.1016/j.carbpol.2012.11.106

Article submitted: July 27, 2018; Peer review completed: December 15, 2018; Revised version received: January 17, 2019; Accepted: January 28, 2019; Published: February 7, 2019.
DOI: 10.15376/biores.14.2.2513-2535